Microstructural Analysis of A Reactive Powder Concrete at Elevated Temperature

D. Erosemiah[1], Dr. N. Sakthieswaran[2], Dr. R. Viji[1]
[1]Department of Civil Engineering, Anna University – BIT Campus, Tiruchirappalli- 620024, TN, India
[2]Department of Civil Engineering, Regional centre of Anna University, Tirunelveli- 627007, TN, India

***Abstract* - Reactive Powder Concrete (RPC) is the ultra-high strength concrete prepared by replacing the ordinary aggregate of normal concrete with quartz powder, zircon sand and steel fibre. In this paper it mainly concern to approach the studies of microstructure of RPC at elevated temperatures. RPC intensified at elevated temperature of about 200 to 800°C to gain excellent mechanical property which is better understandable by performing Scanning Electron Microscope (SEM), Fourier Transform and Infrared Spectroscopy (FTIR) and X-Ray Diffraction (XRD). Particle Size Distribution (PSD) and X-Ray Fluorescence (XRF) are performed in materials to scrutinize the properties of materials. As a result it was concluded that at temperatures 400 and 600°C compressive strength increases gradually in all mixes. Due to influence of high temperature in RPC, crystal hydrate, xonotlite were perceived. At a higher temperature the quality of concrete gradually decreases, acquired by conducting Non Destructive Testing (NDT) (Ultrasonic Pulse Velocity) test.**

Keywords- Reactive Powder Concrete, Elevated temperature, micro structural analysis, compressive strength, NDT.

I. INTRODUCTION

A special amalgamation of constituent materials produces high strength, new generation concrete of Reactive Powder Concrete [RPC]. The composition of reactive powder concrete includes high alumina cement, alccofine, Quartz sand, zircon sand and micro steel fibres. The enhancement of material use, economic benefits and construction of buildings that is strong, durable and sensitive to environment. According to Marcel Chezrey et al [8], high silica fume content and very low water to cement ratio is characterised in RPC to obtain excellent mechanical and durability properties. Microstructure of RPC based on the heat treatment and pressure applied before and during setting. It was observed that the microstructure of CSH hydrate seems to change due to increase in temperature. Ming-Gin Lee et al had evaluated the bond durability and use of RPC as a new repair material to existing concrete. The RPC and steel are found to be more adhesive than other concretes [10].The affiliation of compressive strength with heating temperature of RPC match up to normal concrete, high strength concrete [13].

By changing the proportions of steel fibre(0%,0.5%,1%,1.5%,2%,2.5%) in concrete the relative study of mechanical and durability properties of RPC is inspected [3].The concrete strength in existing building is assessed using a Non destructive technique like rebound hammer and ultra pulse velocity which is in conjunction with destructive techniques. Many factors such as number of cores, variability in concrete strength affects the quality of concrete [7]. The coefficient and law of the size effect of RPC were deliberated through experiments and theoretical analysis [1]. The most notable in RPC containing fibre is the size effect on compressive strength, for a fibre dosage of 0-2% Bezant's size effect formula is preferred to predict the compressive strength of RPC specimens of 100mm.

The bond characteristics of steel fibre in matrix along with bond strength, pullout energy, etc., are presented based on the effect of silica fume. The fibre matrix interfacial properties are enhanced effectively by incorporating various silica fume content ranging from 0% to 40% used in mix proportions, it was found that optimal silica fume dosage of 20% and 30% [15]. This paper outlines the research was started off to direct the micro structural analysis, compressive strength of RPC with varying temperatures with different mix proportions.

II. EXPERIMENTAL PROGRAM

A. Materials

The following are the materials in which RPC is composed of High alumina cement and alccofine as a binder, quartz sand and zircon sand as fine aggregate whereas coarse aggregate is eliminated in this type of concrete and steel fibres are used as admixture to augment the performance of concrete. The required workability is achieved by very low w/b ratio with a high range water reducer Sika Viscocrete. The micro steel fibre of length 13mm and diameter 0.2mm is preferred. The properties of material are obtained by performing X-Ray Fluorescence (XRF) fig. 1 to 4, Particle Size Distribution (PSD) fig. 5 to 8 results and specific gravity of materials is listed below.

Table I Specific Gravity of Materials

Contents	Specific gravity
HAC	3.2
Alccofine	2.9
Quartz sand	2.65
Zircon sand	4.6

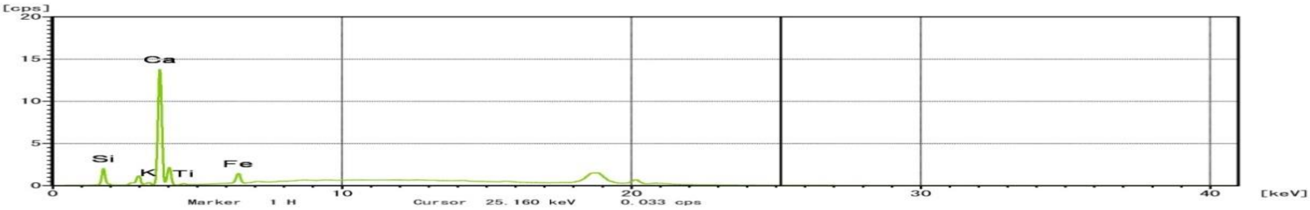

Live time : 60 s Processing Time : P2
XGT Dia. : 100 μm X-ray tube vol. : 50 kV
Current : 1.000 mA
X-ray Filter : Nonexistence Cell : Nonexistence
Quant. Corr. : Standard-less

Elem.	Line	Mass [%]	2sigma [%]	Atomic [%]	Intensity [cps/mA]	Formula	Mass [%]	Molecule [%]
14 Si	K	19.375	0.687	16.642	24.48	SiO2	41.447	40.794
19 K	K	0.903	0.175	0.557	4.37	K2O	1.087	0.683
20 Ca	K	38.437	0.987	23.138	212.91	CaO	53.781	56.718
22 Ti	K	0.716	0.171	0.361	3.13	TiO2	1.195	0.884
26 Fe	K	1.741	0.140	0.752	21.51	Fe2O3	2.490	0.922
8 O		38.828	0.886	58.550				

Fig. 1 XRF of Alccofine

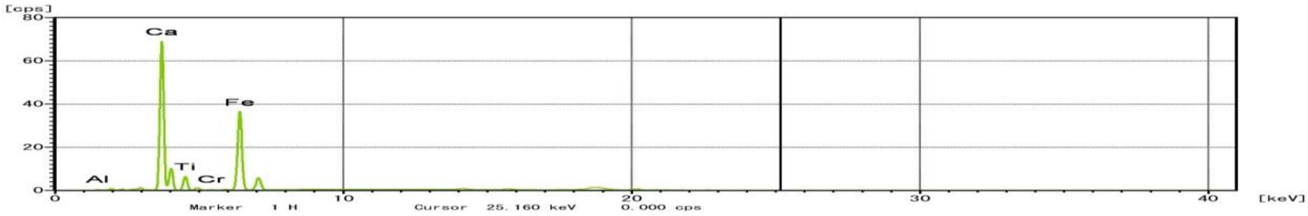

Live time : 60 s Processing Time : P2
XGT Dia. : 100 μm X-ray tube vol. : 50 kV
Current : 1.000 mA
X-ray Filter : Nonexistence Cell : Nonexistence
Quant. Corr. : Standard-less

Elem.	Line	Mass [%]	2sigma [%]	Atomic [%]	Intensity [cps/mA]	Formula	Mass [%]	Molecule [%]
13 Al	K	3.474	0.493	3.605	5.13	Al2O3	6.565	4.564
20 Ca	K	43.242	0.479	30.204	1075.37	CaO	60.505	76.483
22 Ti	K	5.854	0.158	3.421	98.72	TiO2	9.764	8.663
24 Cr	K	0.177	0.036	0.096	4.75	Cr2O3	0.259	0.121
26 Fe	K	16.022	0.224	8.031	629.36	Fe2O3	22.907	10.168
8 O		31.230	0.500	54.643				

Fig. 2 XRF of HAC

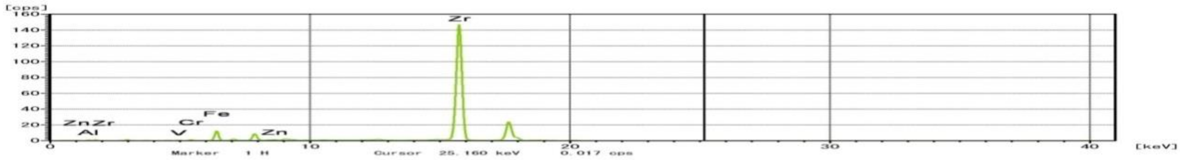

Live time : 60 s Processing Time : P2
XGT Dia. : 100 μm X-ray tube vol. : 50 kV
Current : 1.000 mA
X-ray Filter : Nonexistence Cell : Nonexistence
Quant. Corr. : Standard-less

Elem.	Line	Mass [%]	2sigma [%]	Atomic [%]	Intensity [cps/mA]	Formula	Mass [%]	Molecule [%]
13 Al	K	3.869	0.444	5.405	7.99	Al2O3	7.311	8.803
23 V	K	0.215	0.030	0.159	7.20	V2O5	0.384	0.259
24 Cr	K	0.318	0.030	0.231	13.76	Cr2O3	0.465	0.376
26 Fe	K	2.906	0.060	1.961	205.34	Fe2O3	4.155	3.194
30 Zn	K	0.000	0.019	0.000	0.03	ZnO	0.000	0.000
40 Zr	K	64.913	0.593	26.818	3801.08	ZrO2	87.685	87.367
8 O		27.778	0.448	65.427				

Fig. 3 XRF of Zircon sand

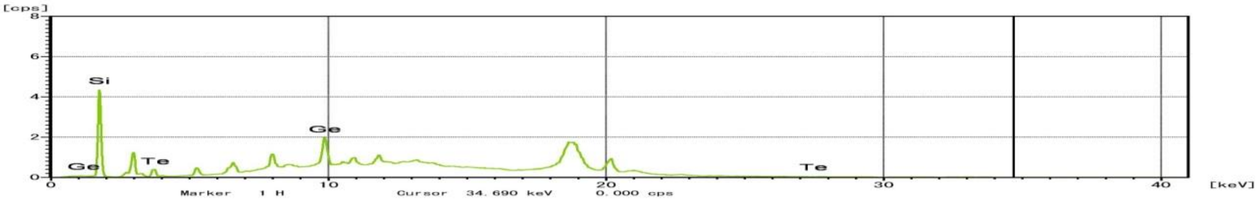

Live time : 60 s Processing Time : P2
XGT Dia. : 100 μm X-ray tube vol. : 50 kV
Current : 1.000 mA
X-ray Filter : Nonexistence Cell : Nonexistence
Quant. Corr. : Standard-less

Elem.	Line	Mass [%]	2sigma [%]	Atomic [%]	Intensity [cps/mA]	Formula	Mass [%]	Molecule [%]
14 Si	K	46.405	0.117	33.194	56.33	SiO2	99.270	99.581
32 Ge	K	0.500	0.050	0.139	25.65	GeO2	0.721	0.416
52 Te	K	0.007	0.193	0.001	0.02	TeO2	0.009	0.003
8 O		53.087	0.143	66.667				

Fig. 4 XRF of Quartz sand

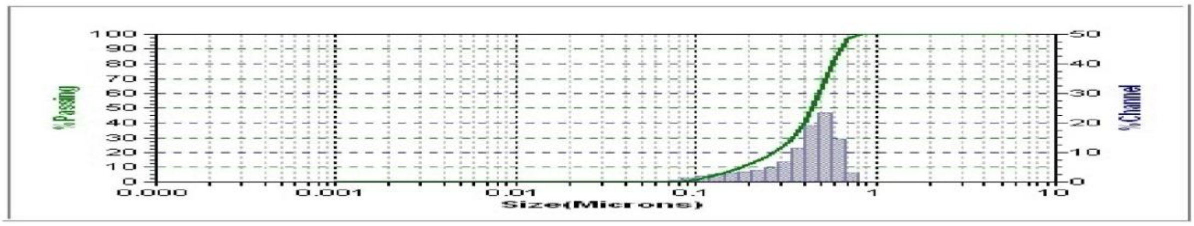

Summary

Data	Value
MI(um):	0.428
MN(um):	0.1607
MA(um):	0.337
CS:	17.80
SD:	0.1754
MW:	2.91E+10
Mz:	0.425
σI:	0.1683
Ski:	-0.21619
Kg:	0.955

Size Percent

Size(um)	%Tile

Percentiles

%Tile	Size(um)
95.00	0.665
90.00	0.623
80.00	0.568
60.00	0.490
50.00	0.452
40.00	0.410
30.00	0.355
20.00	0.2750
10.00	0.1782
5.00	0.1330

Peaks

Dia(um)	Vol%	Width
0.452	100.0	0.35

UDefName	UDefData

Fig. 5 PSD of Alccofine

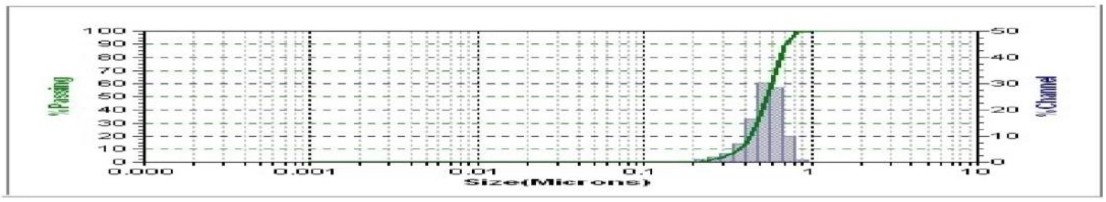

Summary

Data	Value
MI(um):	0.541
MN(um):	0.421
MA(um):	0.508
CS:	11.82
SD:	0.1189
MW:	5.14E+10
Mz:	0.543
σI:	0.1224
Ski:	-0.06589
Kg:	1.068

Size Percent

Size(um)	%Tile

Percentiles

%Tile	Size(um)
95.00	0.736
90.00	0.692
80.00	0.643
60.00	0.576
50.00	0.546
40.00	0.516
30.00	0.484
20.00	0.443
10.00	0.380
5.00	0.320

Peaks

Dia(um)	Vol%	Width
0.546	100.0	0.24

UDefName	UDefData

Fig. 6 PSD of HAC

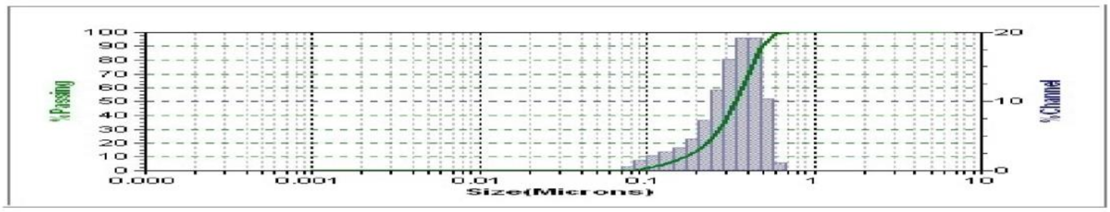

Summary

Data	Value
MI(um):	0.340
MN(um):	0.1663
MA(um):	0.2837
CS:	21.15
SD:	0.1268
MW:	1.28E+10
Mz:	0.340
σI:	0.1244
Ski:	-0.06113
Kg:	0.946

Size Percent

Size(um)	%Tile

Percentiles

%Tile	Size(um)
95.00	0.531
90.00	0.496
80.00	0.448
60.00	0.377
50.00	0.344
40.00	0.310
30.00	0.2745
20.00	0.2323
10.00	0.1690
5.00	0.1280

Peaks

Dia(um)	Vol%	Width
0.344	100.0	0.25

UDefName	UDefData

Fig. 7 PSD of Zircon sand

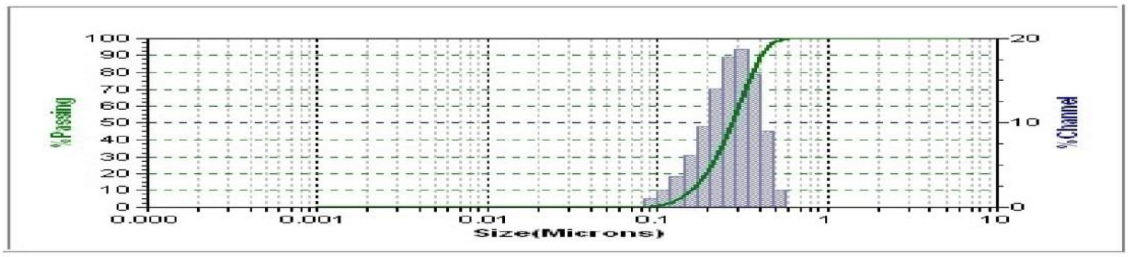

Summary

Data	Value
MI(um):	0.2834
MN(um):	0.1807
MA(um):	0.2480
CS:	24.19
SD:	0.1008
MW:	6.73E+09
Mz:	0.2817
σI:	0.0985
Ski:	0.0817
Kg:	0.937

Size Percent

Size(um)	%Tile

Percentiles

%Tile	Size(um)
95.00	0.452
90.00	0.416
80.00	0.368
60.00	0.304
50.00	0.2774
40.00	0.2517
30.00	0.2254
20.00	0.1964
10.00	0.1598
5.00	0.1344

Peaks

Dia(um)	Vol%	Width
0.2774	100.0	0.20

UDefName	UDefData

Fig. 8 PSD of Quartz sand

B. Mixing proportion

The procedure of mixing RPC is as follows, in first stage dry mixing of ingredients and in the second stage half volume of water having half quantity of super plasticizer is added. The one more ingredient that is steel fibre which is added at the final stage of mixing and mixing time is increased by two minutes from the total mixing duration [17]. The fresh mix of RPC was poured in 150mm cube after mixing and placed on vibration table to remove air voids by compaction. After allowing it to settling for 24 hours, cubes where removed from mould and the kept in curing for 28 days. The mix proportion adopted for RPC is tabulated in Table II.

Table II Mix Proportion of RPC

Mixes	Proportion in %				
	HAC	**Alccofine**	**Quartz sand**	**Zircon sand**	**Steel fibre**
Control mix	100	-	100	-	2
Mix 1	70	30	90	10	2
Mix 2	70	30	80	20	2
Mix 3	70	30	70	30	2
Mix 4	70	30	60	40	2
Mix 5	70	30	50	50	2

III. RESULTS AND DISCUSSION

A. Compressive strength

The fig. 9 shows that the compressive strength is greatest in mix 5 at 200°C which is found to be 55.56 N/mm². The values of mix 1, mix 2, mix 3, mix 4 and mix 5 get increased at 400 and 600°C whereas in control mix the compressive value get decreased at 400 and 600°C compared to 200 and 800°C.In control mix the highest value is obtained at 800°C but it other mixes the lowest value is found to be in 800°C. Mix 3 indicates the increase in compressive values at 200, 400,600 and 800°C compared to other mixes. The value of mix 3 gradually increases from 200°C to 400°C and to 600°C and decreases at 800°C. The optimum value is obtained at temperature 400 and 600°C but exceptionally in mix 5 the optimum value is obtained at 200°C.

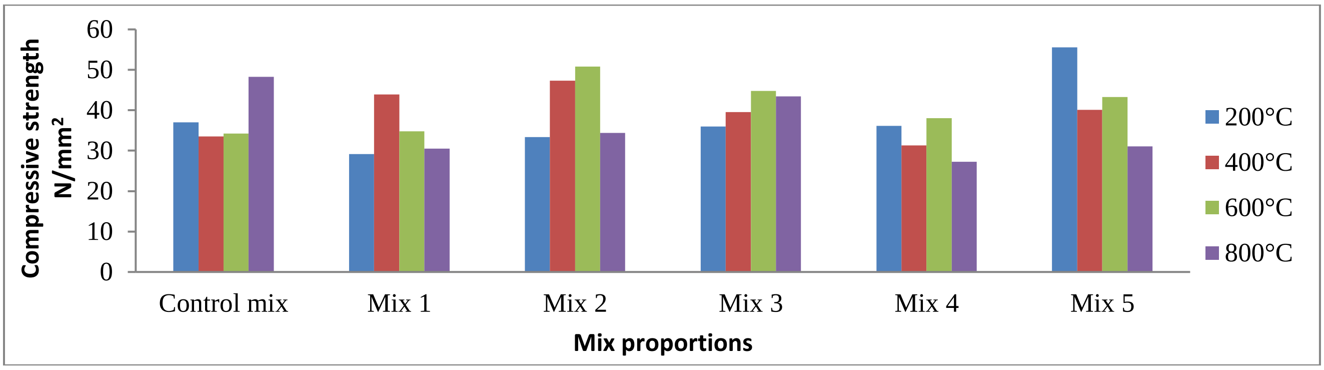

Fig. 9 Compressive strength of mixes at various temperature

B. Ultrasonic pulse velocity

The fig. 10 represents the direct readings of ultrasonic pulse velocity indicates that at 200°C the concrete sample is found to be good because it ranges from 3.5 to 4.5. At 400°C the velocity fluctuates for different mixes as doubtful and medium between <3 and 3 to 3.5 (mix 1 to mix 5), for control mix it is found to be good. For elevated temperature of 600°C, it gradually reduces from good to doubtful. At a higher temperature of about 800°C the quality of concrete is found to be doubtful. The fluctuation occurs in the temperatures 400 and 600°C.The fig. 11 represents the semi direct UPV readings, the quality of concrete is found to be excellent for control mix , mix 1, mix 2 at temperatures 200, 400 and 600°C and at 800°C it is found to be doubtful for all the mixes except mix 3 ,which is medium. At 200°C all the mixes are found to be excellent. For elevated temperature at 400°C the mixes fluctuates from excellent to doubtful. At the temperature of 600°C the velocity gradually decreases from excellent to doubtful. The quality of concrete in mix 5 is doubtful.

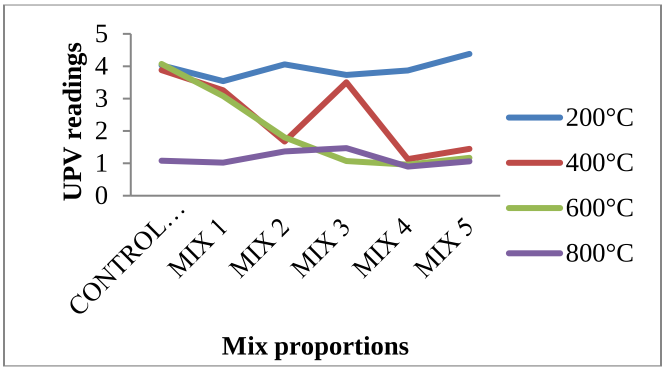

Fig. 10 Direct readings of UPV

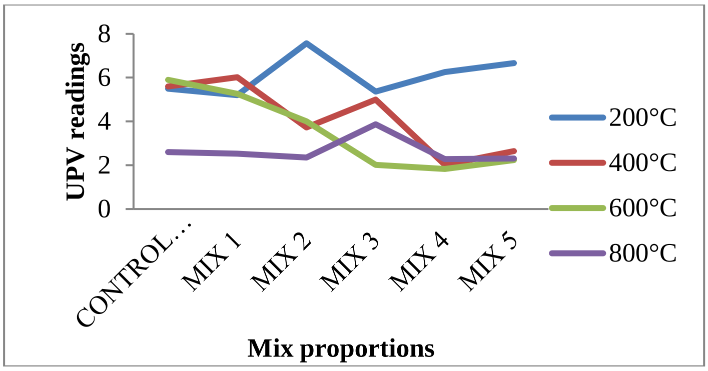

Fig. 11 Semi direct readings of UPV

C. Scanning electron microscope analysis

Scanning Electron Microscope was used to examine the microscopic strength of the RPC specimens before and after experiencing high temperature spalling. In order to investigate the material properties and elemental compositions of the RPCs at elevated temperatures. Fig. 12 represents the SEM images of RPC samples at different temperatures. These images represent the formation of hydrates and unhydrate in the samples. The control mix of RPC at 400°C shows the formation of C-S-H gel and the mix 3 result in the formation of minor cracks on the surface of the concrete at 800°C and also shows that concrete get burnt and the crystal CH is formed. The unhydrated cavities formed over hydrated gives the dense strength of concrete. Formation of ettringite results in the reduction of strength.

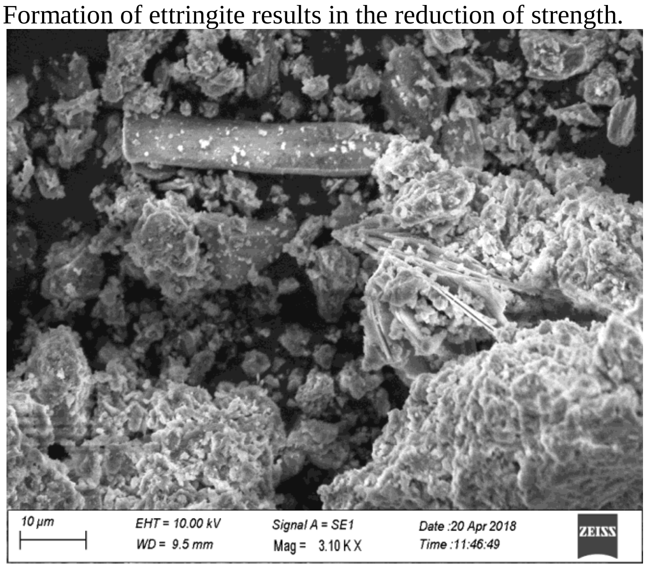

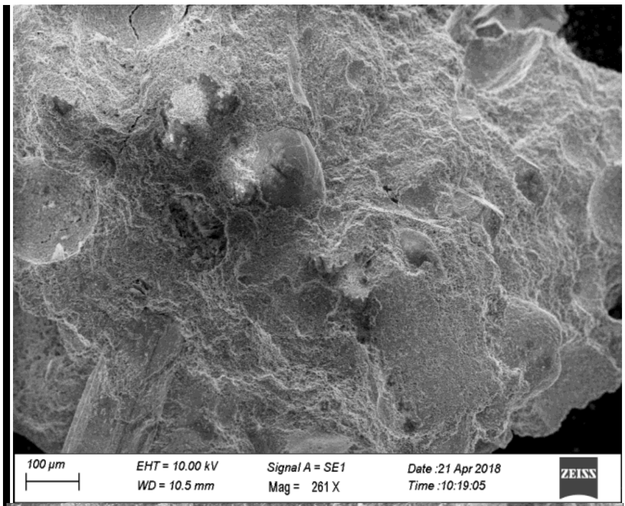

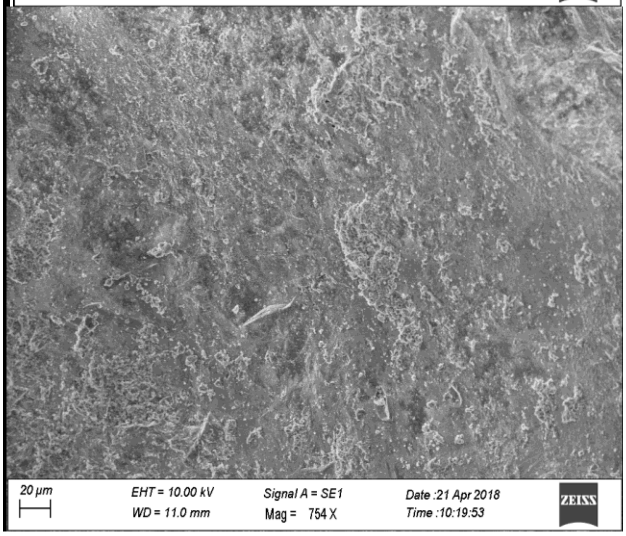

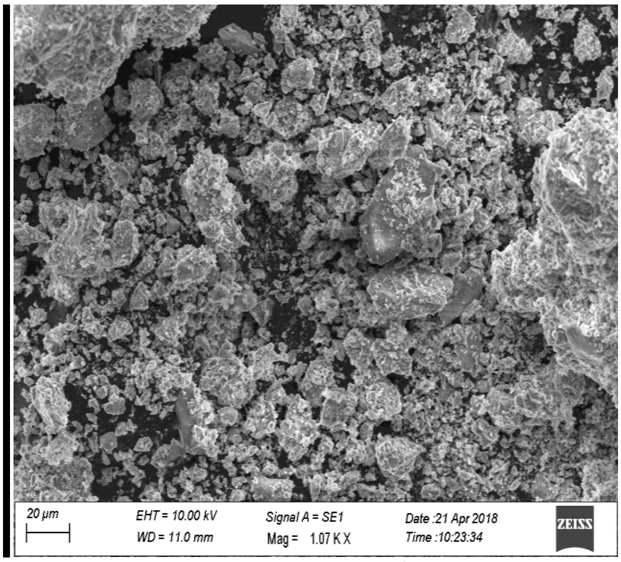

Fig. 12 SEM analysis of RPC

D. Fourier transforms infrared spectroscopy

Fig. 13 to 18 shows that the infrared spectra for control mix, mix 1, mix 2, mix 3, mix 4 and mix 5. Similar vibration bands were observed in all the mixes that are figured below. The infrared spectra of mix had vibration bands at approximately 988 to 992 cm^{-1} associated with the Si-O stretching vibration in the SiO_4 tetrahedral comprising the C-S-H gel. The band observed at 668 cm^{-1} was attributed to the Al-O stretching vibration in AlO_4 groups. The calcite $v_3[CO_3]^{2-}$ vibration bands appeared at 1420 cm^{-1} and the shoulder 880 cm^{-1} associate to $v_2[CO_3]^{2-}$ carbonates. Mixes exhibit IR vibration models at 1651 and 1643 cm^{-1} associated with the bending vibrations of H-OH bonds, related to bound water in the hydrated products formed after alkaline activation.

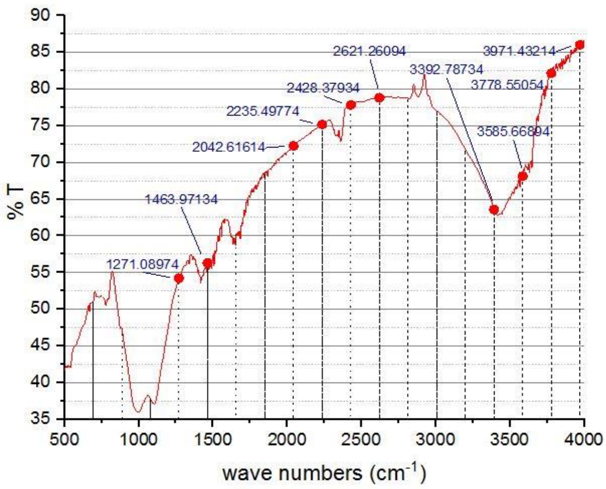

Fig. 13 FTIR analysis of control mix

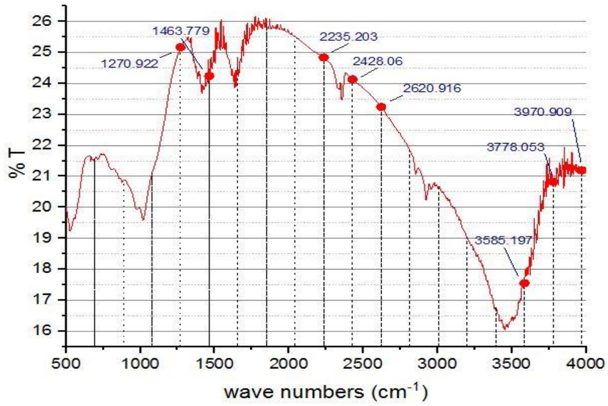

Fig. 14 FTIR analysis of mix 1

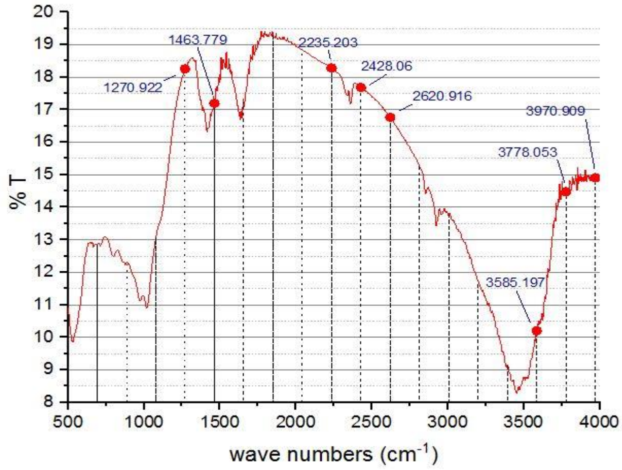

Fig. 15 FTIR analysis of mix 2

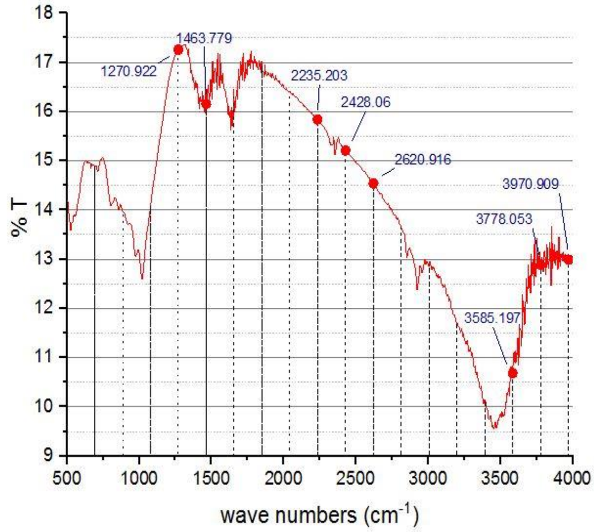

Fig. 16 FTIR analysis of mix 3

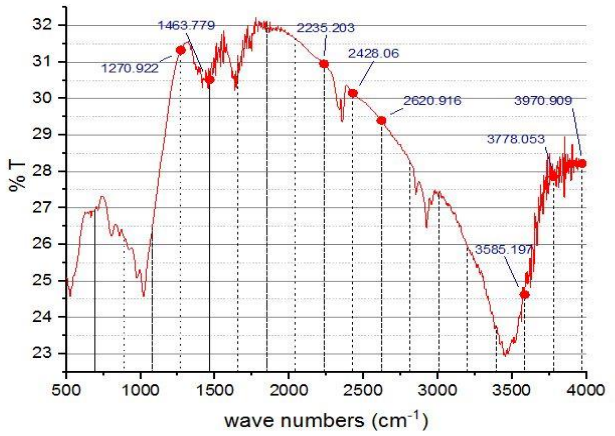

Fig. 17 FTIR analysis of mix 4

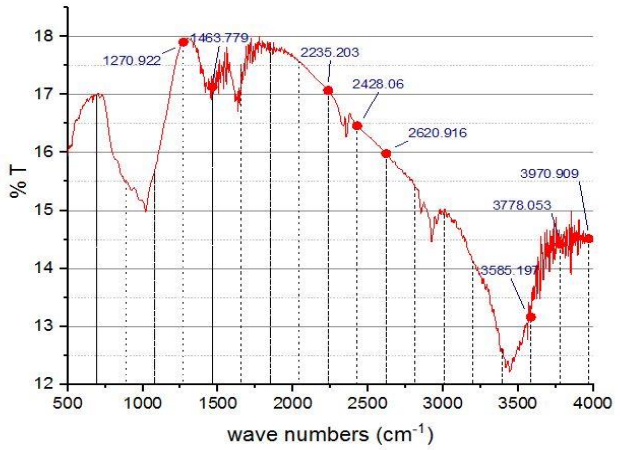

Fig. 18 FTIR analysis of mix 5

E. X ray diffraction

It is used to study the structure, composition, and physical properties of materials. Below fig. 19 to 24 represents the XRD patterns of the hydrated samples C1 (control mix), mix 1, mix 2, mix 3, mix 4 and mix 5 respectively. The XRD analysis for the sample shows the peak value 18° represents the presence of portlandite and the peak value corresponds to 21° and 26° represents the presence of SiO_2.Peak value corresponds to 27,28,31° shows the presence of C_2S because of test carried out on 28 days which gives earlier strength. The value of 30° results in the formation of C-S-H gel formation. The peak values more than 50° is not considered. This result shows that peak values are formed between 25° to 30° indicates the formation of SiO_2 in all the samples.

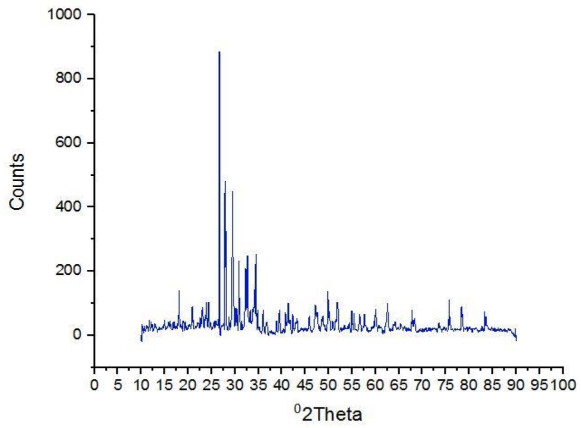

Fig. 19 XRD analysis of control mix

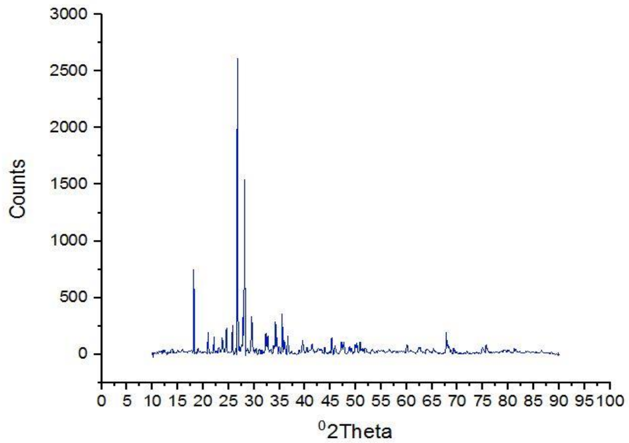

Fig. 20 XRD analysis of mix 1

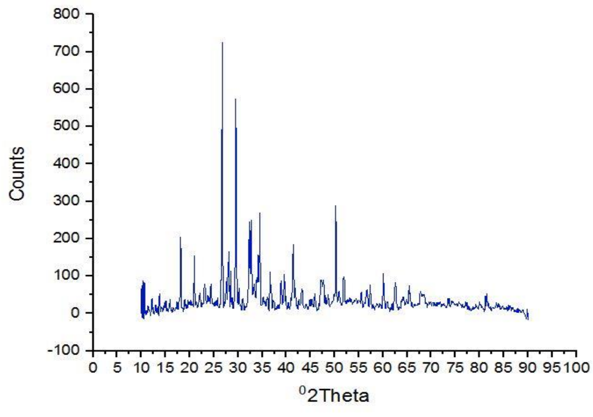

Fig. 21 XRD analysis of mix 2

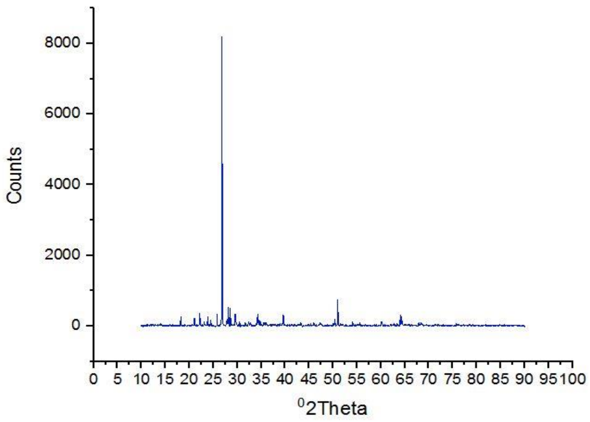

Fig. 22 XRD analysis of mix 3

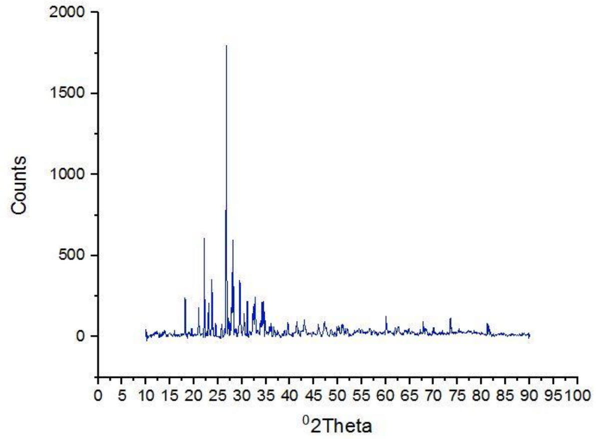

Fig. 23 XRD analysis of mix 4

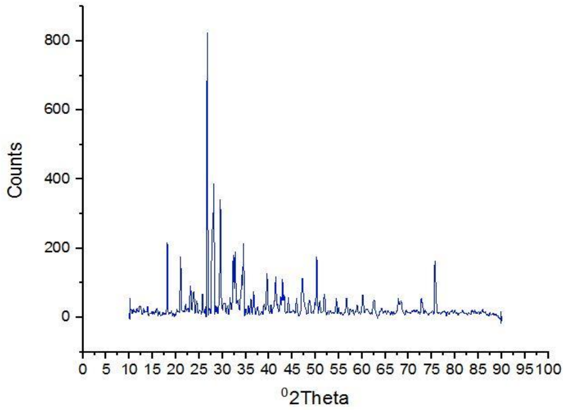

Fig. 24 XRD analysis of mix 5

IV. CONCLUSIONS

The following are the conclusions that are achieved in this project,

- The compressive strength of RPC increases from mix 1 to mix 5 at 200°C and at 400° mix 1 and 2 increases while mix 3, 4 decreases and mix 5 increases. At 600°C mix 1,2 increases but mix 3,4,5 decreases and at 800°C mix 1,2,3 increases whereas mix 4,5 decreases. This result shows that increase in zircon sand as increase in temperature results in decrease in the strength of RPC.
- UPV shows that the quality of concrete is good at 200°C in direct reading. The increase in temperature will results in the poor quality of concrete. In semi direct readings the quality of concrete is found to be excellent for mix 1,2 at 200,400,600°C whereas mix 3,4,5 are found to be doubtful at 600 and 800°C.This result indicates that quality of concrete is good with maximum quartz sand.
- The micro structural studies of RPC show the formation of hydrates and unhydrated clinkers. The C-S-H gel formation indicates the process of hydration and micro cracks are formed in samples at 800°C. The crystals are formed at 400°C in mix 3. Ettringite is not formed. The quality of concrete is found to be good at low temperature; increase in temperature will spoil the quality of concrete.

REFERENCES

[1] An ming zhe, Zhang li jun, Yi Quan xin (2008), ‘Size effect on compressive strength of RPC’, Journal of china university of mining and technology, Vol.18, pp.0279-0282.

[2] Cwirzen A. and Penttala V. et al (2008), ‘Reactive powder based concretes: Mechanical properties, durability and hybrid use with OPC’, Cement and concrete research, Vol.38, pp.1217- 1226.

[3] Deshmukh Rajkumar and Dr.Bage A.A. (2015), ‘Experimental investigation on mechanical and durability properties of RPC’, International Journal of Latest Technology in Engineering, Management & Applied Science, Vol.V, pp.2278-2540.

[4] Halit yazici and Mert yucel yardimci et al (2009), ‘Mechanical properties of RPC containing mineral admixtures under different curing regimes’, Construction and building materials, Vol.23, pp.1223-123.

[5] Halit yazici and Engin deniz (2013), ‘The effect of autoclave pressure, temperature and duration time on mechanical properties of RPC’, Construction and building materials, Vol.42, pp.53-63.

[6] Huseyin yigiter and Serdar aydin et al (2012), ‘Mechanical performance of low cement RPC’, Composites Part B, Vol.43, pp.2907-2914.

[7] Maitham Alwash and Denys Breyss et al (2015), ‘Non Destructive strength evaluation of concrete: Analysis of some key factors using synthetic simulations’, Construction and Building Materials, Vol.99, pp.235-245.

[8] Marcel cheyrezy and Vincent maret et al (1995) , ‘Micro structural Analysis of RPC’, Cement and concrete research, Vol.25, pp.1491-1500.

[9] Mehmet Canbaz (2014), ‘The effect of high temperature on RPC’, Construction and building materials, Vol.70, pp.508-513.

[10] Ming-Gin Lee and Yung-Chih Wang et al (2007), ‘A preliminary study of reactive powder concrete as a new repair material’, Construction and Building Materials, Vol.21, pp.182-189.

[11] Muhammad abid and Xiaomeng hou et al (2017), ‘High temperature and residual properties of RPC – A review’, Construction and building materials, Vol.147, pp.339-351.

[12] Parameshwar N. hiremath and Subhash C. yaragal (2016), ‘Performance evaluation of reactive powder concrete with polypropylene fibers at elevated temperatures’, Construction and Building Materials, Vol.169, pp.499-512.

[13] Wenzhong zheng, Hauyan li, Ying wang (2012), ‘Compressive behavior of hybrid fiber reinforced RPC after high temperature’, Materials and design, Vol.41, pp.403-409.

[14] Wenzhong zheng and Baifu luo (2013), ‘Compressive and tensile properties of RPC with steel fibers at elevated temperatures’, Construction and building materials, Vol.41, pp.844-851.

[15] Yin wen chan and Shu Hsien chu (2004), ‘Effect of silica fume on steel fiber bond characteristics in RPC’, Cement and concrete research, Vol.34, pp.1167-1172.